Fachtagung "Experimentelle Strömungsmechanik"
5.–7. September 2023, München

Exploiting the full potential of deep neural networks for PIV applications

Esther Lagemann, Wolfgang Schröder, Christian Lagemann

Lehrstuhl für Strömungslehre und Aerodynamisches Institut, RWTH Aachen University, Wüllnerstraße 5a, 52062 Aachen

Neuronale Netze, Optical flow, Turbulenzspektra, turbulente Kanalströmung
Neural networks, Optical Flow, turbulence spectra, turbulent channel flow

Abstract

Experimental studies of turbulent wall-bounded flows are often desired to capture the complete spectrum of turbulent scales across the entire wall-normal direction. Achieving this objective in a single measurement is typically challenging if not impossible at moderate and high Reynolds numbers since the field of view required to capture the large-scale motions contradicts the resolution necessary to adequately resolve the small-scale flow structures. Moreover, standard cross-correlation based PIV evaluation routines further reduce the spatial resolution of the acquired particle images since they require finite-size interrogation windows for the velocity estimation. However, the introduction of a deep learning based optical flow estimator called Recurrent All-pairs Field Transforms-PIV (RAFT-PIV) (Lagemann et al. 2021a, 2022a) solves this resolution reduction drawback of traditional methods by operating on the original image resolution, i.e., RAFT-PIV provides a velocity vector for each pixel. We will demonstrate that the increased spatial resolution has the potential to simultaneously capture the large-scale flow features in the outer flow field and the velocity distribution close to the wall, i.e., in the buffer layer and the viscous sublayer, within the same measurement setup. Precisely, this ability is shown with a wall-normal PIV setup covering the complete channel half height of a turbulent channel flow at $Re_\tau \approx 1100$. Based on a combination of experimental and open-source DNS data, we will demonstrate that RAFT-PIV can be used to estimate relevant turbulence statistics, e.g., stresses and energy spectra, accurately - even in close vicinity to the wall where established cross-correlation based PIV tools usually become unreliable.

Introduction

In the past few years, several algorithms have been proposed that leverage deep learning techniques within the data analysis workflow of particle-image velocimetry (PIV) experiments (Cai et al. 2019, Lagemann et al. 2019, Zhang and Piggot 2020). This emerging body of work has shown that deep learning has the potential to match or outperform state-of-the-art classical algorithms in terms of efficiency, accuracy, and spatial resolution. Due to the significance of PIV experiments, progress in PIV processing approaches, which leverage state-of-the-art artificial intelligence (AI) tools, impacts a wide range of problems in applied physics and engineering where velocity components of flow fields need to be determined. These methods sidestep the problem of manually designing an analytic pipeline by defining an end-to-end network whose output is the dense per-pixel optical flow field. Thus, fine flow structures can be resolved which are typically smoothed by traditional cross-correlation based methods due to the inherent spatial averaging. One promising approach is a deep learning based method called RAFT-

GALA e.V., Karlsruhe, Germany, ISBN 978-3-9816764-9-5

PIV which is inspired by the recently introduced RAFT backbone (Teed and Deng 2020). RAFT-PIV is a neural optical flow estimator which is specifically designed for the use case of PIV images. It is unique in the sense that it operates entirely on a specific input resolution and updates iteratively its flow predictions. In the methodological paper (Lagemann et al. 2021a), RAFT-PIV was shown to achieve a new state-of-the-art accuracy on a public PIV database and to outperform available supervised and unsupervised learning based approaches by a large margin. Its tremendous success based on a superior generalization ability was demonstrated for a series of different datasets that allow robust conclusions to be drawn on the utility of deep learning for PIV analysis (Lagemann et al. 2021b, 2022a, 2022b). However, a general lack of confidence in novel deep learning based processing methods still exists within a majority of the experimental fluids community.

Hence, this work ultimately has two intertwined goals: (1) to evidence the generalization and usefulness of our neural RAFT-PIV approach in challenging real-world applications to enhance the general confidence in neural processing approaches amongst practitioners, and, (2) to demonstrate the tremendous potential of deep optical flow methods in deriving important turbulence statistics such as stresses and energy spectra - especially in near-wall regions governed by strong velocity gradients which are typically challenging for cross-correlation based approaches.

To this end, we also present how accurate instantaneous wall-shear stress distributions can be derived from such measurements using the linear relationship between inner-scaled velocity and wall-normal position in the viscous sublayer. This is in contrast to traditional approaches like the Clauser chart method (Clauser 1956) or the single-pixel ensemble correlation (Westerweel 2004) which only provide time-averaged quantities. To summarize, we will take advantage of the full potential of neural optical flow techniques in PIV applications to demonstrate that these methods provide reliable flow field information which will support turbulence research and help to validate large-scale numerical simulations.

The paper is organized as follows: We first introduce the experimental setup and complementary direct numerical simulation (DNS) data. Then, we present an extensive body of empirical work exploiting the full potential and superior performance of RAFT-PIV in PIV processing. Finally, we close with concluding comments.

Experimental setup and benchmark DNS data

The experiments are performed in an Eiffel-type wind tunnel at the Institute of Aerodynamics at RWTH Aachen University. A 9000 mm long inlet section with a tripping device provides a fully developed, turbulent channel flow (TCF) in the 2700 mm long measurement section, which is shown in figure 1. It features an aspect ratio of $AR = 20$ with a cross-section of $100\,\mathrm{mm} \times 2000\,\mathrm{mm}$ (channel half height $2h$ × width w) that ensures a negligible influence of three-dimensional effects. Comparisons to DNS data (Schäfer et al. 2011) verify the quality of the provided fully developed TCF. For the TCF measurements at a friction Reynolds number of $Re_\tau \approx 1100$, the two-dimensional two-

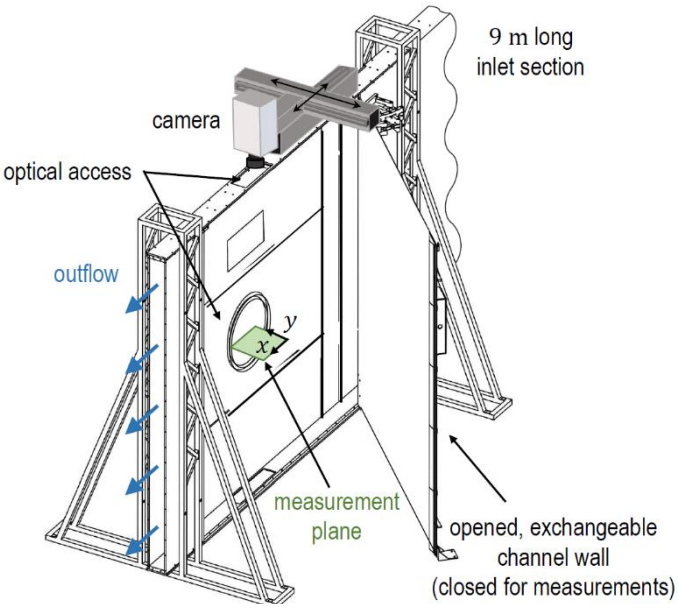

Figure 1: Measurement section of the TCF facility

GALA e.V., Karlsruhe, Germany, ISBN 978-3-9816764-9-5

component PIV setup is realized with a Darwin Duo 40 laser and a Photron SA3 camera equipped with a Tamron 180 mm lens. The input image size of this test case is $1024\ \mathrm{px} \times 1024\ \mathrm{px}$ and the camera operates at a frame rate of 1000 Hz.

The DNS data used for validating the TCF measurement is provided by the *Johns Hopkins Turbulence Databases* (Li et al. 2008) and is publicly available. In the following, some computational details of this simulation are provided, but we refer the interested reader to the original publication of Graham et al. (2016) for a comprehensive data description. The released DNS data contain a turbulent wall-bounded flow with periodic boundary conditions in the longitudinal and transverse directions, and no-slip conditions at the top and bottom walls. In this simulation, the Navier-Stokes equations are solved using a wall–normal, velocity–vorticity formulation (Kim et al. 1987). Solutions of the governing equations are provided using a Fourier-Galerkin pseudo-spectral method for the longitudinal and transverse directions and a seventh-order Basis-splines (B-splines) collocation method in the wall normal direction. The simulation is performed for approximately a single flow through time. The velocity vector and pressure fields are stored every five time steps resulting in 4000 data extracts. The computational domain measures $\mathrm{L_x} \times \mathrm{L_y} \times \mathrm{L_z} = 8\pi\,\mathrm{h} \times 2\,\mathrm{h} \times 3\pi\,\mathrm{h}$. The numerical grid contains $\mathrm{N_x} \times \mathrm{N_y} \times \mathrm{N_z} = 2048 \times 512 \times 1536$ grid points and the numerical time step is $\Delta t = 0.0013$ in dimensionless units. The friction Reynolds number is $Re_\tau \approx 1000$, i.e., a bit lower than in the experimental measurements.
Apart from validation, the DNS data additionally provide the underlying flow field of synthetic particle images. Such synthetic data are necessary to assess the capability of RAFT-PIV in accurately predicting instantaneous flow quantities. This property cannot be validated based on real experimental data since they do not possess an instantaneous ground truth for comparison. To generate synthetic particle images, the velocity fields from those simulations need to be transferred onto an equidistant grid as they have a non-equidistant grid spacing in the wall-normal direction. The chosen discretization has a spatial resolution of $\Delta x^+ = \Delta y^+ = 1$ such that an adequate resolution of the near-wall flow field is provided. These interpolated velocity fields are referred to as ground truth data and build the basis for the particle image generation using the approach described in Lagemann et al. (2021a).

Results

This section is divided into two parts which present results of synthetic and real-world PIV measurements of a TCF, respectively. Synthetic PIV images root on snapshots of the DNS data and serve the purpose of enabling a direct comparison of the RAFT-PIV output to realistic ground truth data relative to both, time-averaged flow quantities and instantaneous results. Since no ground truth distributions exist for the experimental data, we compare the time-averaged flow quantities obtained via RAFT-PIV to DNS data and analytic solutions. Under conditions where a standard PIV processing tool, can provide meaningful results, e.g., the wall-normal velocity profile, we also present the respective data obtained from our in-house PIV evaluation tool Pascal-PIV (Marquardt et al. 2019).

Synthetic PIV images
We start with a comparison of the time-averaged wall-normal velocity profile scaled by inner units as shown in figure 2. Both methods, the cross-correlation (Pascal-PIV) and the optical-flow (RAFT-PIV) based approach, match the trend of the underlying DNS (ground truth) closely for $\mathrm{y}^+ > 10$. More importantly, however, the figure shows that an established cross-correlation

GALA e.V., Karlsruhe, Germany, ISBN 978-3-9816764-9-5

based technique is not able to resolve the transition between the log layer and the viscous sublayer for this setup since it possesses only a single velocity vector in this region. In contrast, RAFT-PIV captures the distribution within the buffer layer and the viscous sublayer remarkably well and resolves even the closest location to the wall ($y^+ = 0.5$) accurately demonstrating its tremendous high-resolution advantage. Precisely, since RAFT-PIV outputs a velocity vector for each image pixel individually, the spatial resolution can be increased by at least a factor of eight which is particularly helpful in near-wall regions as indicated in figure 2.

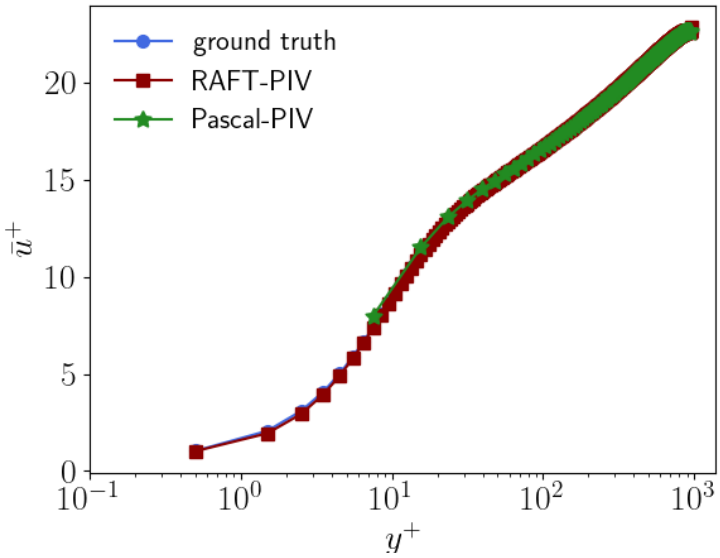

Figure 2: Inner-scaled velocity profile $\boldsymbol{u}^+$ of the synthetic PIV images as a function of the wall-normal coordinate $\boldsymbol{y}^+$.

This advantage becomes even more prominent when deriving higher-order turbulence statistics such as stresses and energy spectra. A respective side-by-side comparison can be found in figures 3 and 4. Similar to the previous finding one can note that both methods, i.e., RAFT-PIV and Pascal-PIV, match the ground truth well for $y^+ > 300$. For smaller y^+ values, however, the cross-correlation based competitor features partially severe deviations and underestimates the normal and shear stresses substantially. This is a well-known issue of traditional PIV methods attributed to the spatial averaging/windowing inherent to the algorithm itself. That is, only one displacement vector can be computed per interrogation window yielding a smoothed flow field. As a result, small flow structures are filtered out – although sophisticated state-of-the-art image deformation and predictor/corrector schemes are applied in this work. In contrast, results obtained by RAFT-PIV match the ground truth accurately along the entire wall-normal direction and even resolve smallest spatial structures precisely. This superior spatial resolution ability is also convincingly demonstrated in the pre-multiplied energy spectra which are shown for two y^+ locations in figure 4. The RAFT-PIV results nicely follow the ground truth distribution with only some slight deviation in the smallest wavelength range. Similar to the previous findings, a cross-correlation based counterpart can only cover the rough trend of the ground truth energy spectrum and substantially underestimates the small wavelength regime.

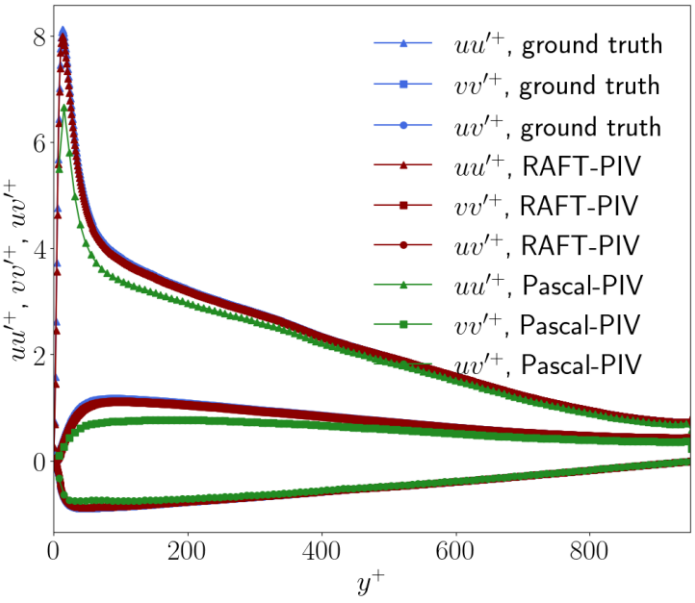

Figure 3: Shear stresses scaled by inner units of the synthetic TCF PIV images as a function of the wall-normal coordinate y^+.

GALA e.V., Karlsruhe, Germany, ISBN 978-3-9816764-9-5

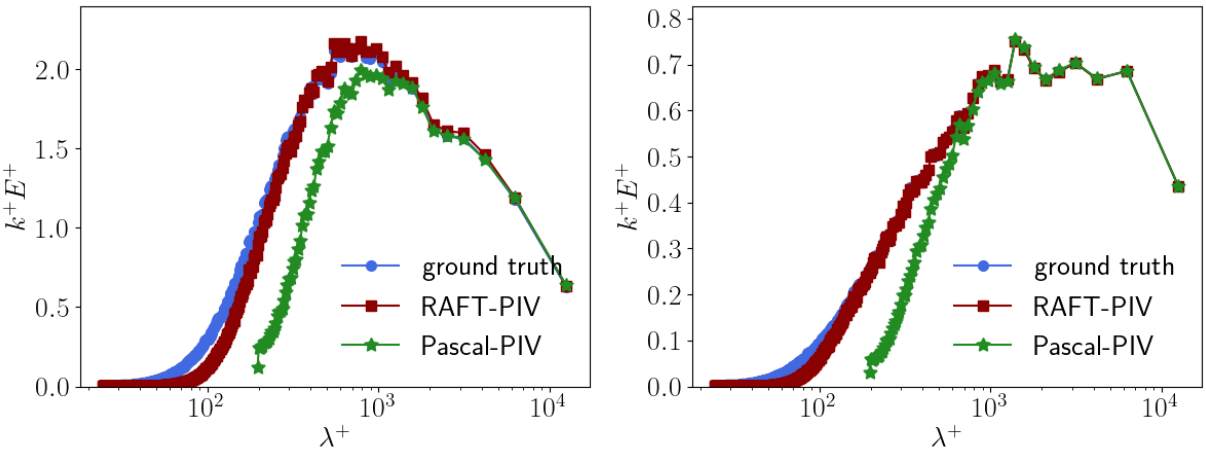

Figure 4: Pre-multiplied streamwise energy spectra by inner units of the synthetic PIV images as a function of the wavelength λ^+ at two wall-normal locations. Left: $y^+ = 15$, right: $y^+ = 150$.

Another major advantage of the superior spatial resolution ability of RAFT-PIV manifests in the derivation of near-wall flow quantities such as the friction velocity u_τ and the wall-shear stress τ_w, which, in contrast to most of the other experimental techniques, can be derived in an instantaneous and time-averaged fashion over the entire spatial dimension captured in the image without any further assumptions. Given RAFT-PIV results of the present setup, the instantaneous wall-shear stress can be calculated from the linear relation between inner-scaled velocity and wall-normal position in the viscous sublayer $u^+ = y^+$ such that $\tau_w = u\,\eta/y$, where u denotes the streamwise velocity component, η the dynamic viscosity, and y the wall-normal position in physical units. To increase the accuracy of the wall-shear stress, a wall-shear stress value is calculated with each velocity value within the viscous sublayer and subsequently averaged. In this setup, the viscous sublayer is captured by five pixels, i.e., five velocity estimates are provided via RAFT-PIV. Evaluating the synthetic particle images of the TCF with RAFT-PIV, the temporally and spatially averaged wall-shear stress deviates by only 0.009 % from the original ground truth value demonstrating its high level of accuracy. More importantly, however, RAFT-PIV further provides the possibility to extract the wall-shear stress from instantaneous snapshots individually, which - to the best of our knowledge - is hardly possible with any other method for such a large region of interest. Figure 5 depicts an example of the instantaneous wall-shear stress distribution. RAFT-PIV nicely captures the ground truth distribution with very little deviations.

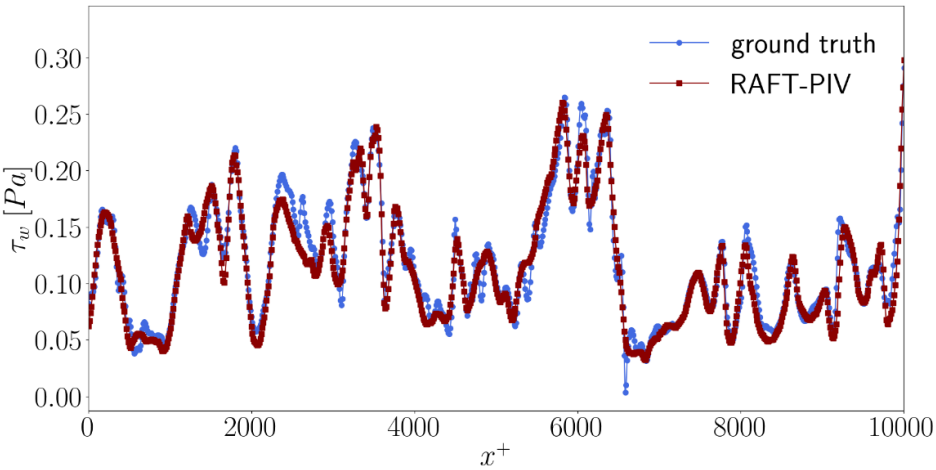

Figure 5: Wall-shear stress prediction of an instantaneous image pair of the synthetic PIV images as a function of the streamwise coordinate x^+.

GALA e.V., Karlsruhe, Germany, ISBN 978-3-9816764-9-5

Experimental measurements

Next, we demonstrate the superior performance of RAFT-PIV on a set of PIV images acquired under real measurement conditions. These potentially include uncertainties such as measurement noise, reflections at the wall, sensor pollution, and/or imperfect estimation of the correct Reynolds number and consequently, of the nominal wall-shear stress value, due to an improper calibration or an incorrect determination of the exact temperature during the measurements. For these conditions, figure 6 depicts a time-averaged velocity profile obtained by RAFT-PIV in comparison to the cross-correlation based counterpart and complementary DNS data. RAFT-PIV and Pascal-PIV match the DNS data for moderate and large wall distances $y^+ > 10$. In the near-wall region ($y^+ < 10$), however, exclusively RAFT-PIV estimates precise velocity values. Naturally, slight deviations due to measurement uncertainties occur in the viscous sublayer but the superior spatial resolution ability of the deep optical flow network facilitates velocity predictions in regions which could not be resolved thus far. In this context, please note that these measurements are not fine-tuned to investigate near-wall flow regions like the buffer and the viscous sublayer but the complete channel half height. As a consequence, the viscous sublayer is only captured by three pixels while displacement prediction is impeded due to inhomogeneous particle distributions. Considering these fundamental challenges, the results depicted in figure 6 become even more remarkable and evidence the noteworthy generalization ability and robustness of RAFT-PIV.

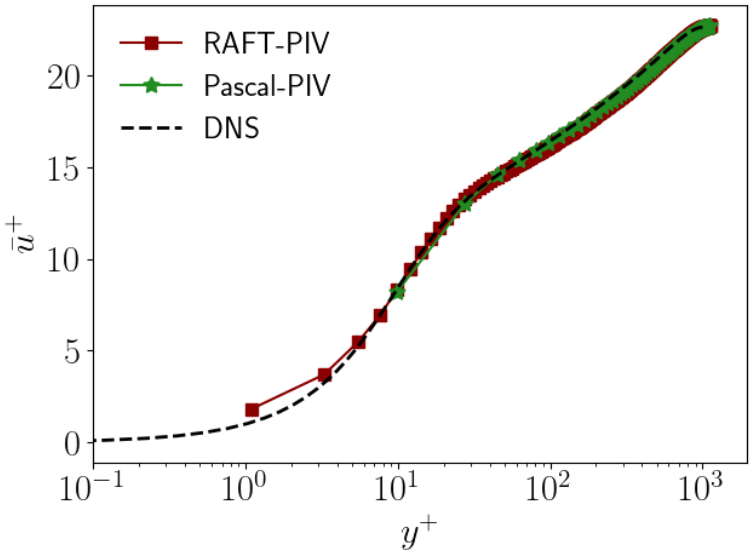

Figure 6: Inner-scaled velocity profile $\boldsymbol{u}^+$ of the experimental PIV images as a function of the wall-normal coordinate $\boldsymbol{y}^+$.

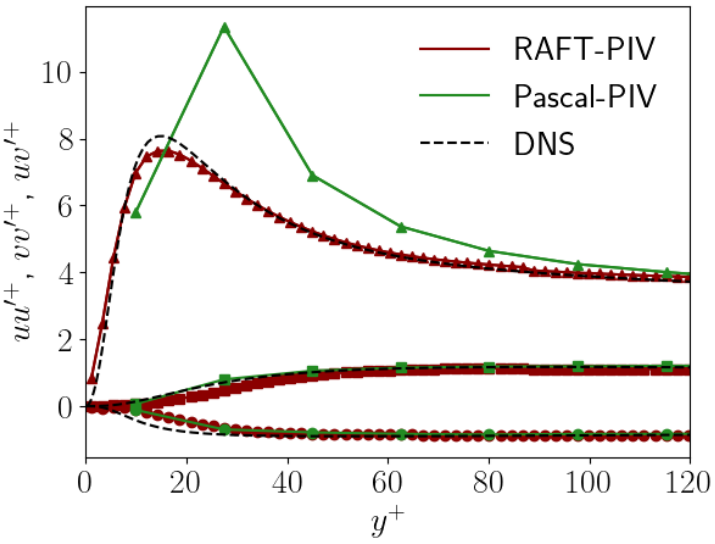

Figure 7: Shear and normal stresses in inner units of the experimental PIV images as a function of the wall-normal coordinate y^+.

In line with the previous section presenting stress profiles of synthetic PIV images, figure 7 shows shear and normal stresses of the experimental data. A close-up of the inner layer is given to highlight that an established cross-correlation based method matches the complementary DNS data distribution well only for $y^+ > 100$. Substantial deviation occurs in the near-wall region, especially for the streamwise velocity component. In contrast, our deep optical flow predictor closely follows the DNS curve. More importantly, this holds for regions which are not resolved by standard PIV methods such as the inner peak in the streamwise stresses.

GALA e.V., Karlsruhe, Germany, ISBN 978-3-9816764-9-5

Finally, we compute the instantaneous and time-averaged wall-shear stress distributions for the experimental data. In this setup, the viscous sublayer is captured by three pixels, i.e., three velocity estimates are provided via RAFT-PIV. Averaging the resulting wall-shear stress values in the streamwise direction and over time yields $\tau_w = 0.135$ Pa. The theoretical value for this flow based on analytical calculation (Pope 2000) measures $\tau_w = 0.127$ Pa. Hence, the experimentally obtained value deviates by about 6.2 % - most likely due to measurement uncertainties such as imperfect inflow conditions and slightly deviating fluid properties. Figure 8 depicts the derived wall-shear stress distribution of an instantaneous snapshot. Although no ground truth is available for comparison, the general trend resides in the same magnitude range as the complementary DNS and closely matches the standard deviation of the wall-shear stress values. Considering all previous results, we therefore conclude that also the instantaneous wall-shear stress predictions are reliable.

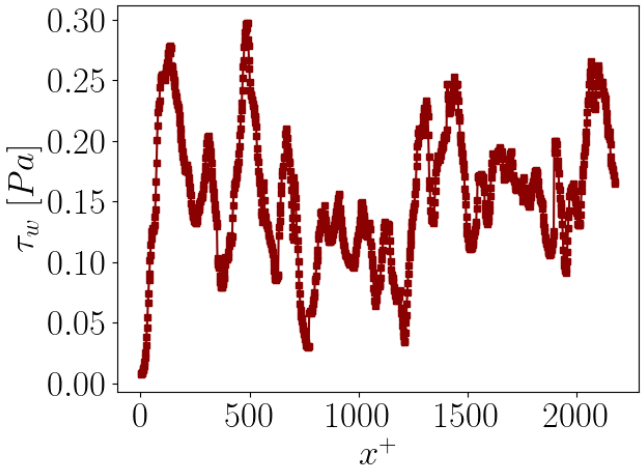

Figure 8: Wall-shear stress prediction of an instantaneous image pair of the experimental PIV images as a function of the streamwise coordinate x^+.

Conclusion

The present investigation leverages the full potential of deep learning based optical flow techniques for PIV applications. We highlight that our deep-learning based approach RAFT-PIV enables an accurate computation of relevant flow quantities such as shear stresses and energy spectra from velocity predictions in regions where established methods typically fail due to unresolved scales and strong velocity gradients. Moreover, it is shown how the spatially developing wall-shear stress distribution is obtained solely based on wall-normal particle images. Since RAFT-PIV does not rely on averaged displacement vectors within finite-size interrogation windows like traditional PIV evaluation tools, it provides a velocity vector for each pixel. Thus, several data points within the viscous sublayer can easily be obtained from a high-resolution PIV measurement and the linear relationship between the inner-scaled velocity and the wall-normal position can be used to calculate the instantaneous wall-shear stress. The evaluation of synthetic and experimental particle images of a TCF at $Re_\tau \approx 1100$ convincingly demonstrates the validity of the resulting instantaneous and time-averaged wall-shear stress distributions.

Considering these aspects, we strongly believe that deep optical flow methods such as RAFT-PIV constitute a major step for the majority of PIV measurements and facilitate numerous novel analysis possibilities of existing datasets, especially in regions which are usually not resolved by cross-correlation based counterparts such as the viscous sublayer and the lower buffer layer in turbulent wall-bounded flows.

GALA e.V., Karlsruhe, Germany, ISBN 978-3-9816764-9-5

Acknowledgement

This research was funded by the Deutsche Forschungsgemeinschaft within the research project “Learning Deep Optical Flow Estimation for Particle-Image Velocimetry” (DFG SCHR 309/79). The authors gratefully acknowledge the Gauss Centre for Supercomputing e.V. for funding this project by providing computing time on the GCS Supercomputers.

References

Lagemann, C., Lagemann, K., Mukherjee, S. & Schröder, W. (2021a): “Deep recurrent optical flow learning for particle image velocimetry data”. Nature Machine Intelligence 3, 641–651.

Lagemann, C., Lagemann, K., Mukherjee, S. & Schröder, W. (2022a): “Generalization of deep recurrent optical flow estimation for particle-image velocimetry data”. Measurement Science and Technology 33, 094003.

Cai, S., Zhou, S., Xu, C. & Gao, Q (2019): “Dense motion estimation of particle images via a convolutional neural network”. Experiments in Fluids 60, 73.

Lagemann, C., Lagemann, K., Schröder, W. & Klaas, M. (2019): ”Deep artificial neural network architectures in PIV applications” in *13th InternationalSymposium on Particle Image Velocimetry*.

Zhang, M. & Piggott, M. D (2020): “Unsupervised Learning of Particle Image Velocimetry”. arXiv preprint *arXiv:2007.14487*.

Teed, Z. & Deng, J. (2020): “RAFT: Recurrent all-pairs field transforms for optical flow” in *Computer Vision–ECCV 2020: 16th European Conference*, 402–419.

Lagemann, C., Klaas, M. & Schröder, W (2021b): “Unsupervised Recurrent All-Pairs Field Transforms for Particle Image Velocimetry” in *14th International Symposium on Particle Image Velocimetry*.

Lagemann, C., Mäteling, E., Klaas, M. & Schröder, W (2022b): “Analysis of PIV Images of Transonic Buffet Flow by Recurrent Deep Learning Based Optical Flow Prediction” in *20th International Symposium on Applications of Laser and Imaging Techniques to Fluid Mechanics*.

Clauser, F. H. (1956): “The turbulent boundary layer”. Advances in Applied Mechanics 4, 1–51.

Westerweel, J., Geelhoed, P. & Lindken, R. (2004): “Single-pixel resolution ensemble correlation for micro-PIV applications”. Experiments in Fluids 37, 375–384.

Li, Y., Perlman, E., Wan, M., Yang, Y., Meneveau, C., Burns, R., Chen, S., Szalay, A. & Eyink, G. (2008): “A public turbulence database cluster and applications to study Lagrangian evolution of velocity increments in turbulence”. Journal of Turbulence, N31.

Graham, J., Kanov, K., Yang, X. I. A., Lee, M., Malaya, N., Lalescu, C. C., Burns, R., Eyink, G., Szalay, A. & Moser, R.D. (2016): “A web services accessible database of turbulent channel flow and its use for testing a new integral wall model for LES”. Journal of Turbulence 17, 181–215.

Kim, J., Moin, P. & Moser, R. (1987): “Turbulence statistics in fully developed channel flow at low Reynolds number”. Journal of Fluid Mechanics 177, 133–166.

Marquardt P., Klaas M., and Schröder W. (2019) “Experimental investigation of isoenergetic film-cooling flows with shock interaction”. AIAA Journal 57:3910–3923

Pope, S. B. (2000): “Turbulent flows”. Cambridge University Press.

GALA e.V., Karlsruhe, Germany, ISBN 978-3-9816764-9-5